ARMY RESEARCH LABORATORY

Surface Enhanced Raman Scattering (SERS)-Based Next Generation Commercially Available Substrate: Physical Characterization and Biological Application

by Mikella E. Hankus, Dimitra N. Stratis-Cullum and Paul M. Pellegrino

ARL-RP-0335 **September 2011**

A reprint from the *SPIE-Optics and Photonics West,* volume 8099, paper 8099-7, San Diego, CA, 20 August 2011.

NOTICES

Disclaimers

The findings in this report are not to be construed as an official Department of the Army position unless so designated by other authorized documents.

Citation of manufacturer's or trade names does not constitute an official endorsement or approval of the use thereof.

Destroy this report when it is no longer needed. Do not return it to the originator.

Army Research Laboratory
Adelphi, MD 20783-1197

ARL-RP-0335 **September 2011**

Surface Enhanced Raman Scattering (SERS)-Based Next Generation Commercially Available Substrate: Physical Characterization and Biological Application

Mikella E. Hankus, Dimitra N. Stratis-Cullum and Paul M. Pellegrino
Sensors and Electron Devices Directorate, ARL

A reprint from the *SPIE-Optics and Photonics West,* volume 8099, paper 8099-7, San Diego, CA, 20 August 2011.

REPORT DOCUMENTATION PAGE

Form Approved
OMB No. 0704-0188

1. REPORT DATE *(DD-MM-YYYY)*	2. REPORT TYPE	3. DATES COVERED (From - To)
September 2011	Reprint	

4. TITLE AND SUBTITLE
Surface Enhanced Raman Scattering (SERS)-Based Next Generation Commercially Available Substrate: Physical Characterization and Biological Application

5a. CONTRACT NUMBER

5b. GRANT NUMBER

5c. PROGRAM ELEMENT NUMBER

6. AUTHOR(S)
Mikella E. Hankus, Dimitra N. Stratis-Cullum and Paul M. Pellegrino

5d. PROJECT NUMBER

5e. TASK NUMBER

5f. WORK UNIT NUMBER

7. PERFORMING ORGANIZATION NAME(S) AND ADDRESS(ES)
U.S. Army Research Laboratory
ATTN: RDRL-SED-D
2800 Powder Mill Road
Adelphi, MD 20783-1197

8. PERFORMING ORGANIZATION REPORT NUMBER
ARL-RP-0335

9. SPONSORING/MONITORING AGENCY NAME(S) AND ADDRESS(ES)

10. SPONSOR/MONITOR'S ACRONYM(S)

11. SPONSOR/MONITOR'S REPORT NUMBER(S)

12. DISTRIBUTION/AVAILABILITY STATEMENT
Approved for public release; distribution unlimited.

13. SUPPLEMENTARY NOTES
A reprint from the *SPIE-Optics and Photonics West*, volume 8099, paper 8099-7, San Diego, CA, 20 August 2011.

14. ABSTRACT
The development of a sensing platform capable of detecting and identifying hazards including biological, chemical, and energetic in nature is a long sought after goal of the Army and many other first responders. Surface enhanced Raman scatting (SERS) is one spectroscopic technique gaining popularity as a solution to many sensing needs due to its many advantages such as high sensitivity, little to no sample preparation required, and use in numerous environmental settings). Despite all the advantages of SERS, it still remains a marginalized sensing technique primarily due to the challenges in fabricating a reliable, highly sensitive and reproducible nanoscale surface. In this work, we show that many of these challenges have been overcome with a newly developed commercially available Klarite SERS substrate. These substrates are fabricated in a fashion similar to standard Klarite substrates, but due to changes in size and spacing of the inverted pyramidal structurethere is an overall increase of SERS sensing capabilities of up to 4 orders of magnitude. In this proceeding paper, the next generation Klarite (308 and 309) substrates are characterized, analyte sensitivity demonstrated at 633 nm and 785 nm, and a brief discussion of their biological sensing capabilities is presented.

15. SUBJECT TERMS
Surface enhanced Raman scattering, Raman, SERS, substrate, biological, energetic, hazard, Klarite

16. SECURITY CLASSIFICATION OF:			17. LIMITATION OF ABSTRACT	18. NUMBER OF PAGES	19a. NAME OF RESPONSIBLE PERSON
a. REPORT	b. ABSTRACT	c. THIS PAGE			Mikella E. Hankus
Unclassified	Unclassified	Unclassified	UU	16	19b. TELEPHONE NUMBER (*Include area code*) (301) 394-0948

Surface enhanced Raman scattering (SERS)-based next generation commercially available substrate: physical characterization and biological application

Mikella E. Hankus, Dimitra N. Stratis-Cullum and Paul M. Pellegrino
US Army Research Lab, 2800 Powder Mill Rd., Adelphi, MD 20783

ABSTRACT

The development of a sensing platform capable of detecting and identifying hazards including biological, chemical, and energetic in nature is a long sought after goal of the Army and many other first responders. Surface enhanced Raman scatting (SERS) is one spectroscopic technique gaining popularity as a solution to many sensing needs due to its many advantages such as high sensitivity, little to no sample preparation required, and use in numerous environmental settings). Despite all the advantages of SERS, it still remains a marginalized sensing technique primarily due to the challenges in fabricating a reliable, highly sensitive and reproducible nanoscale surface. In this work, we show that many of these challenges have been overcome with a newly developed commercially available Klarite SERS substrate. These substrates are fabricated in a fashion similar to standard Klarite substrates, but due to changes in size and spacing of the inverted pyramidal structurethere is an overall increase of SERS sensing capabilities of up to 4 orders of magnitude. In this proceeding paper, the next generation Klarite (308 and 309) substrates are characterized, analyte sensitivity demonstrated at 633 nm and 785 nm, and a brief discussion of their biological sensing capabilities is presented.

Keywords: Surface enhanced Raman scattering, Raman, SERS, substrate, biological, energetic, hazard, Klarite

1. INTRODUCTION

The development and widespread use of sensing schematics for dynamic real time detection of hazardous materials, chemical, biological and energetic in nature, is a perpetual goal in numerous fields of research. An ideal sensor can be used in a host of different environments, is sensitive to several types of target analytes at low concentrations, can be used in a quantitative manner, is cost efficient, is small, requires little to no sample preparation, and is commercially available. To both the United States Army and first responders such an ideal sensor would be advantageous allowing for the rapid detection and identification of hazardous materials before or after exposure to human populations. To answer this need, several sensing schematics have been proposed and developed. Some of the more common and effective hazard sensing technologies are based on vibrational spectroscopy. In the sensing community, there is increased interest in using commercially available surface enhanced Raman scattering- based substrates for detection due to many of the advantages of this technology.

Vibrational-based spectroscopic techniques rely on specific vibrations in a molecule from which a fingerprint spectrum can be generated for qualitative and quantitative measurements. Raman and Raman-based vibrational spectroscopic-based schematics offer many sensing advantages. Raman and Raman-based techniques are particularly well suited for the identification and characterization of unknown targets both hazardous and benign.[1-6] Raman is particularly advantageous as it (i) does not suffer from interferences from water, (ii) requires little to no sample preparation, (iii) is robust and can be used in numerous environments, (iv) is relatively insensitive to the wavelength of excitation employed and (v) produces a narrow-band spectral signature unique to the molecular vibrations of the analyte. All of these advantages contribute to Raman spectroscopy's capability to perform sample characterization, identification and quantification. Despite such advantages, however, Raman spectroscopy has remained a marginalized technique for trace detection of hazardous materials in the field, mainly due to the extremely low scattering cross sections characteristic to many hazards.

Surface enhanced Raman scattering (SERS) is a technique that overcomes the shortcomings of spontaneous Raman by greatly enhancing Raman scattering, which has been reported to detect a single molecule under ideal conditions.[7-9] Compared to conventional Raman, the SERS enhancement has been reported to be as much as 14 orders of magnitude

greater, although it is most commonly observed on the order of six to eight orders of magnitude. The SERS phenomenon observed is mainly attributed to two main mechanisms (i) the electromagnetic fields generated at or near nanostructured surfaces and (ii) the physical or chemical adsorption of the analyte to a surface. SERS has the potential to serve as a rapid screening tool for many types of hazardous materials. SERS has already been shown to be a viable sensing technique for chemical, biological and energetic hazard detection.[6, 10-15]

Despite the many advantages of SERS, application to real-world situations remain challenging mainly due to the difficulties in fabricating highly sensitive and spectrally/physically reproducible SERS substrates. Specifically SERS challenges are found in achieving a reproducible and a uniformly roughened nanoscale substrate from which repeatable SERS signal measurements can be collected. To meet the reproducibility and sensitivity challenge, several SERS platforms have been demonstrated (colloids, film over nanospheres, fiber optic bundles, nanoparticles, lithographically produced structures). At best, some of these substrate platforms generally have 15% relative standard deviation (RSD; the measure of the reproducibility of an analysis) from substrate-to-substrate and SERS signal enhancements of 7 to 8 orders of magnitude.[16, 17] Consequently, many research groups and companies have focused concerted efforts toward increasing the enhancement ability, reproducibility, and mass production of substrates. For the Army and first responders, such a substrate platform with increased sensitivity and reliability would be very advantageous.

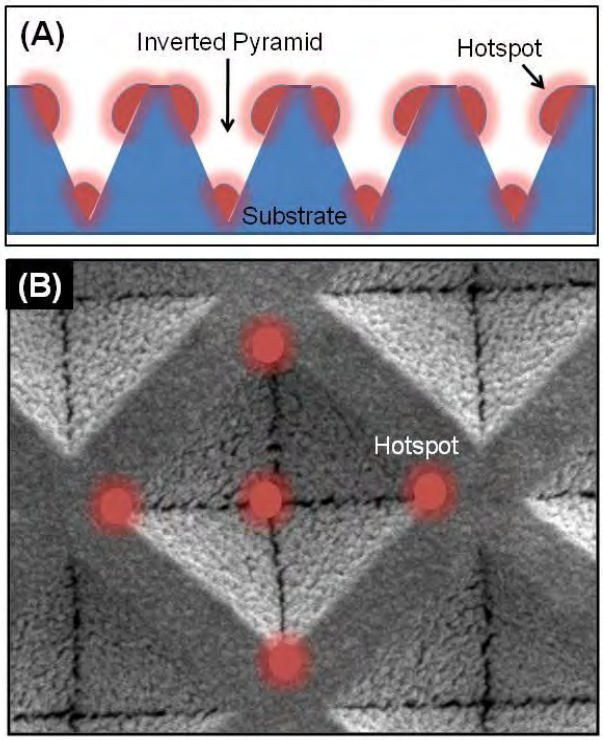

Figure 1. Schematic demonstrating location of hotspots across Klarite surface. In (A) a cartoon rendering displays hot spots as being located at the bottom of the inverted pyramids and at the sides. In (B) and top down SEM image with theorized hot spot location displayed.

Some success fabricating and applying uniform SERS substrates has been demonstrated with commercially available Klarite™ substrates (D3 Technologies Ltd.).[18-22] These substrates were developed using Si-based semiconductor fabrication techniques.[22] Klarite substrates are fabricated using a well defined Silicon fabrication technique in which a silicon diode mask is defined by optical lithography, and then KOH surface etched. The process results in an array of highly reproducible inverted pyramid structures.[22] These array pyramids are reported to have "hot spots" or "trapped plasmons" located inside the wells.[22] In Figure 1, a schematic of a theorized hot spot model is shown from a side view (A) and top down approach (B).[10, 20, 22, 23] In this Figure hot spots (not drawn to scale) are theorized to be located at the bottom of the inverted pyramid wells, as well as at the sharp points of the inverted pyramid base. These substrates have been previously characterized by our group using AFM analysis and plasmon data collection. From our previous work[24], AFM images have been used to characterize inverted pyramids of approximately 1.47 um in width, and 1 um in

depth. These substrates have plasmon absorbance bands are located at 577 nm and 749 nm, thus demonstrating the usefulness of this substrate with a range of excitation sources. Additionally, due to the fabrication process used, under ideal conditions these substrates have demonstrated typical RSDs ranging from 10-15% under drop and dry conditions.

While these standard Klarite substrates do demonstrate a high degree of substrate reproducibility and very low substrate background (SERS signal and surface morphology) for applications to real-world situations increased analyte sensitivity is still necessary. Towards this end, newer prototype Klarite based substrates have been fabricated. The morphologies of these substrates dramatically differ in overall shape, pitch and spacing as compared to the standard Klarite substrate resulting in very interesting sensing capabilities.

In these proceedings, we will report on the characterization, reproducibility and limit of detection results of next generation Klarite substrates using trans-1,2-bi-(4-pyridyl) ethylene (BPE), and collection data using the 633 nm and 785 nm lasers of a Renishaw Raman Microscope. Some preliminary biological data will also be presented for spore detection on the different substrates.

2. EXPERIMENTAL

2.1 Substrates

Commercially available slide mounted Klarite™ 302 SERS substrates were purchased from D3 Technologies Ltd. Slides were individually wrapped and vacuum sealed. The SERS active area on these slides was a small 4 mm x 4 mm wafer with a gold surface. The standard Klarite™ slides were only used once and opened just prior to measurement to reduce any possible surface fouling. Additionally, the substrate was submerged in ethanol to remove any possible dust that may have accumulated on the surface. Next generation Klarite substrates (designated as 308's and 309's) were used as received from D3 following the same procedures used for the standard substrates. Due to a limited number of substrates available, data were collected using a standard addition method. Typically in SERS data collection on the standard and 308 substrates five measurements across the substrate surface were measured, due to the limited active area on the 309's two measurements were collected per quadrant. Most data in these proceedings will be presented as an average of a collected data set and the standard deviation error shown, unless otherwise indicated.

2.2 Instrumentation

All plasmon data were obtained using an Avantes system. The system is controlled using AvantesSpec software. Data analysis is performed using Igor Pro 4.0 (WaveMetrics, Inc.). Unless otherwise indicated data acquisition parameters were: 500 ms exposure time, for 10 accumulations, and 3 averages. Using this methodology a total of five spectra were collected from each substrate.

Scanning electron microscope (SEM) images were obtained using a FEI environmental SEM (Quanta 200 FEG).

A Renishaw in Via Reflex Raman microscope was used for SERS and Raman spectra collection. Spectra were collected using the NIR 785 nm laser. The laser light was focused onto the sample using a 5X objective, exposures were 10 seconds in length, and 3 accumulations was collected per spot. Approximately 7 mW of power irradiated the surface of the substrate. Five spectra were collected from each substrate. Samples were positioned using a motorized XYZ translational stage internal to the microscope. Spectra were collected, and the instrument was run using Wire 3.2 software operating on a dedicated computer. Data analysis was achieved using IgorPro 6.0 software (Wavemetrics).

2.3 Chemicals

Chemicals used included trans-1,2-bi-(4-pyridyl) ethylene (BPE) and ethanol (EtOH). All chemicals were used as received without further purification. The SERS response test protocol used a modified standard addition methodology developed (in partnership with Edgewood Chemical Biological Center) and commonly used for SERS DARPA evaluation program. Briefly, in these experiments the substrate was soaked in 5 mL of a BPE/EtOH solution for 10 minutes to insure complete binding of the BPE with the surface, and then the SERS spectra of the substrate were collected from five different points across the substrate (while still in solution). Once the measurements were collected, the old solution was removed and the substrate was soaked in the next concentration of BPE/EtOH solution. Following this protocol, typical BPE solution concentration additions included: Blank none, EtOH, $1x10^{-14}$, $1x10^{-13}$, $1x10^{-12}$, $1x10^{-11}$, $1x10^{-10}$, $5x10^{-10}$, $1x10^{-09}$, $5\ x10^{-09}$, $7.5\ x\ 10^{-09}$, $1\ x10^{-08}$, $2.5\ x\ 10^{-08}$, $5\ x10^{-08}$, $7.5\ x\ 10^{-08}$, $1\ x10^{-07}$, $2.5\ x\ 10^{-07}$, $5\ x10^{-07}$, $7.5\ x\ 10^{-07}$, $1\ x10^{-06}$ M BPE, for a total of 20 measurements.

2.4 Biological samples

Spore suspension *B. coagulans (ATCC SUS-CG)* was purchased from Raven Biologicals and used at a log 4 or 6 population per 0.1 mL of solution. For experiments in this report, a 1 uL aliquot of spore suspension was drop dried onto the active area of the Klarite substrate. Once the suspension had completely dried, SERS measurements were collected. Due to the nature of the drop dry technique,[24] uneven coverage of the spore samples did occur with a higher concentration being located around the "edge" of the coffee ring. To compensate for this, multiple measurements were collected towards the "center" of each analyte ring on the substrate surface.

3. RESULTS AND DISCUSSION

3.1 Physcial Characterization

Standard Klarite and next generation Klarite substrates were first characterized by SEM image analysis. In Figure Figure 2, a visual schematic of standard Klarite and next generation Klarite substrates is shown. In Figure 2A, a cartoon of a typical Klarite substrate is demonstrated with the Klarite chip called out for clarity. In Figure 2B the sensing area for the three different types of substrate is shown. Klarite 302 and 308 are both composed of a single uniform sensing area, while Klarite 309 consists of four different quadrants. In Figure 2C, a modified SEM image demonstrates the different measurements on the substrate, (i) inner (active) and outer (overall area) portion of an inverted pyramid, (ii) outer length of a pyramid, and (iii) inner length of a pyramid. All of these measurements are used for determination of the standard sensing area per inverted pyramid (calculations assumes planar surface for ease), and the overall percentage of active sensing area per chip. Planar surface calculations are being used to observe trending, additional work with AFM analysis will be conducted to determine an actual area calculation.

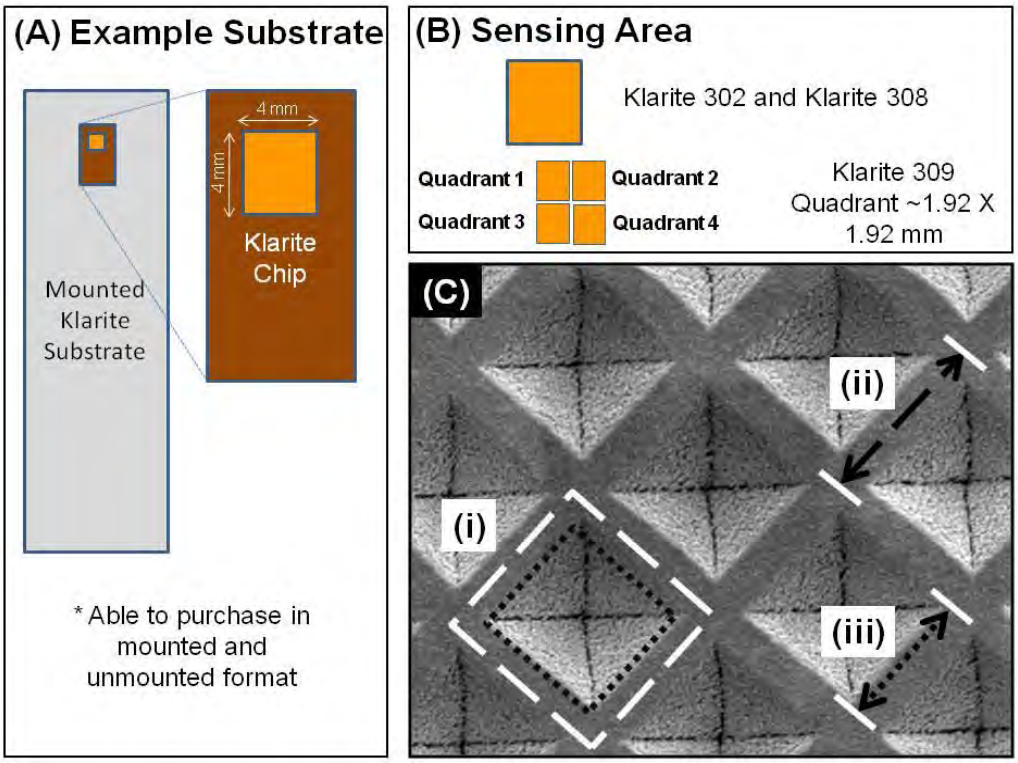

Figure 2. Visual schematic of standard Klarite and next generation Klarite substrates. In (A) a cartoon of a typical Klarite substrate is demonstrated with the Klarite chip called out for clarity. In (B) the sensing area for the three different types of substrate is shown. Klarite 302 and 308 are both composed of a single uniform sensing area, while Klarite 309 consists of four different quadrants. In (C) a modified SEM image demonstrates the different measurements on the substrate, (i) inner and outer portion of an inverted pyramid, (ii) outer length of a pyramid, and (iii) inner length of a pyramid

Using SEM analysis the sizes of inverted pyramids for the different Klarite substrates were determined, see Figure 3 for an example SEM of a Klarite 309 substrate. The overall pyramid area of the outer pyramid, inner (active) pyramid, and lengths of each measurement are shown in Figure 2C. To compare the different types of substrates, a general overall activity factor (K) was defined as active area of chip (for measurements considered same area of 0.0160 m^2) / total area of a single pyramid (m^2) x % of single pyramid that is active. Using SEM analysis, a standard Klarite substrate has an outer width of about 2040 nm, and an inner pyramid width of 1470 nm, for a total sensing area of 51.93% of a single pyramid. Assuming an overall active chip size of 4 mm x 4 mm, the total number of cells for each substrate is around 3.84 x 10^6. The standard Klarite has an overall F comparison number of 0.12. The Klarite 308 has an outer width of 636.4 nm, and an inner pyramid width of about 454.0 nm, for a total sensing area of 51.0% of a single pyramid. Assuming an overall active chip size of 4 mm x 4 mm, the total number of cells for each substrate is around 3.95 x 10^7. The Klarite 308 has an overall F comparison number of 1.26. The Klarite 309 Quadrant 1 substrate has an outer width of about 758.1 nm, and an inner pyramid width of 580.0 nm, for a total sensing area of 58.7%. Assuming an overall active chip size of 1.92 mm x 1.92 mm, the total number of cells for each substrate is around 6.41 x 10^6. The Klarite 309 Quadrant 1 has an overall F comparison number of 1.02. The Klarite 309 Quadrant 2 substrate has an outer width of about 806.5 nm, and an inner pyramid width of 484.0 nm, for a total sensing area of 36.0%. Assuming an overall active chip size of 1.92 mm x 1.92 mm, the total number of cells for each substrate is around 5.67 x 10^6. The Klarite 309 Quadrant 2 has an overall F comparison number of 0.55. The Klarite 309 Quadrant 3 substrate has an outer width of about 790.3 nm, and an inner pyramid width of 661.0 nm, for a total sensing area of 70.0%. Assuming an overall active chip size of 1.92 mm x 1.92 mm, the total number of cells for each substrate is around 5.09 x 10^6. The Klarite 309 Quadrant 3 has an overall F comparison number of 1.12. The Klarite 309 Quadrant 4 substrate has an outer width of about 806.5 nm, and an inner pyramid width of 564.0 nm, for a total sensing area of 49.0%. Assuming an overall active chip size of 1.92 mm x 1.92 mm, the total number of cells for each substrate is around 5.67 x 10^6. The Klarite 309 Quadrant 4 has an overall F comparison number of 0.75.

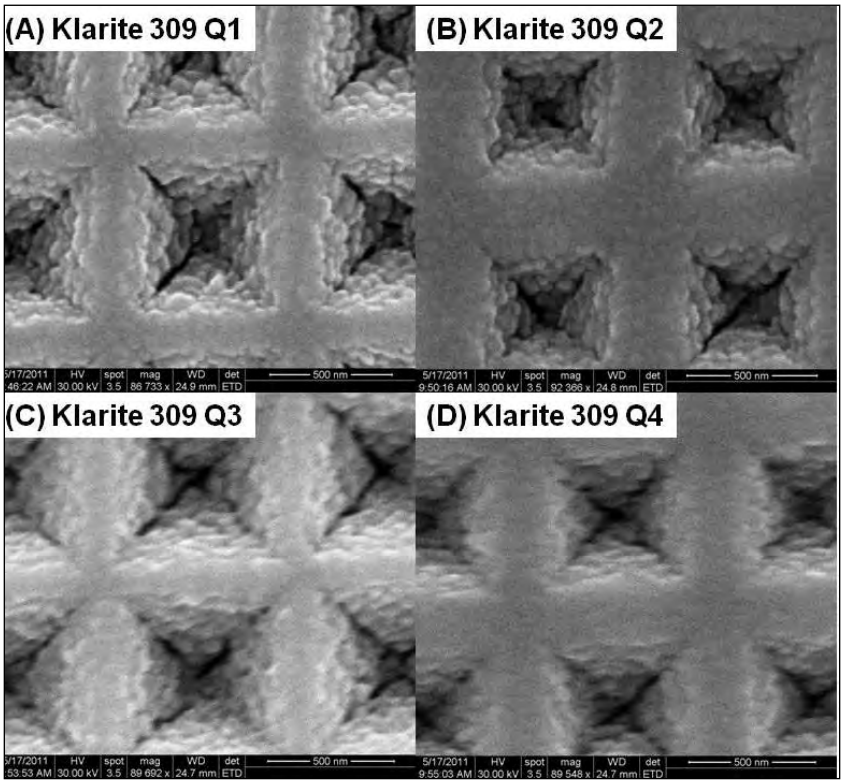

Figure 3. Example SEM images of different quadrants of Klarite 309 substrate.

Due to the differences in overall chip size the Klarite 302 and 308 will be compared, and the different quadrants of the 309 will be compared. Comparing overall pyramid size, it can be seen that the standard Klarite is almost 10X larger than the 308, however comparing density values, the Klarite 302 is almost 10X less dense. Taking into account the density X % active area/pyramid (and applying a K factor), we see that the 308 is almost 10.5 times larger, see F comparison. We expect due to these different in density, there would be even more active hot spots across the 308 as compared to the standard Klarite, however additional modeling work will have to be to conclusively determine this. Ranking (largest to smallest) % area active/ per pyramid of the different quadrants of the Klarite 309, it is observed that quadrant 3 is largest, followed by quadrant 1, followed by quadrant 4, and last is quadrant 2. Looking at the F comparison, trending from largest to smallest is quadrant 3, quadrant 1, quadrant 4 and then quadrant 2. This data suggests that quadrant 3 might be more SERS active as compared to the other quadrants.

Table 1. Comparison of standard Klarite, Klarite 308 and Klarite 309 quadrants as determined by SEM analysis.

Substrate Type	Outer width (nm)	Inner width (nm)	% area active/ per pryamid	Active chip area in (m^2)	Density (actual chip area)	Density X % active (normalized to same 4 mm X 4 mm chip area)	F Comparison
Klarite 302	2040	1470	51.9	1.60E-05	3.84E+06	1.25E+19	0.12
Klarite 308	636	454	51.0	1.60E-05	3.95E+07	1.26E+20	1.26
Klarite 309 Q1	758	580	58.7	3.69E-06	6.41E+06	1.02E+20	1.02
Klarite 309 Q2	806	484	36.0	3.69E-06	5.67E+06	5.54E+19	0.55
Klarite 309 Q3	790	661	70.0	3.69E-06	5.90E+06	1.12E+20	1.12
Klarite 309 Q4	806	564	49.0	3.69E-06	5.67E+06	7.53E+19	0.75

3.2 Determination of detection capabilities

Limits of detection and overall typical signal to noise (SN) ratios were determined following the DARPA SERS BPE testing evaluation previously described and briefly outlined in the experimental section. For these experiments two different wavelengths were evaluated to determine if the location of the plasmon band would influence the overall SERS response of the substrates. As a reminder, surface plasmon data has previously indicated that absorbance max for the different substrates are as follows: standard klarite substrate at 577 nm and 749 nm, Klarite 308 at 590 nm and 675 nm, and for Klarite 309 quadrant 1 has plasmon bands located at 723 nm and 840nm, quadrant 2 has plasmon bands located at 700 nm and 831 nm, quadrant 3 has plasmon absorbance bands located at 734 nm and 845 nm, and quadrant 4 has plasmon absorbance bands located at 713 nm and 836 nm. The SN ratios and error were calculated for all substrate types over 20 different calculations and at two different wavelengths. An example of data analysis is shown in Figure 4A. In Figure 4A, an example of results from a standard Klarite substrate, collected with 785 nm laser, averaged data points with SN >3, error represents 1 std. dev. In this data set the R^2 value observed is 0.941. Using this type of analysis, it was possible to calculate the sensitivity for all substrate types at the two different wavelengths, see Table 2 for a summary of results. Figure 4B shows an example average SN for different quadrants of Klarite 309. It should be noted that this LOD is analyte specific, as different chemical interactions between the surface and the analyte can occur by changing the identity of the chemical of interest. From the results shown in Table 2, it can be clearly seen that Klarite 308 can be used for detecting the lowest concentrations of BPE, for an overall improvement of almost four orders

of magnitude under some conditions. From the characterization data discussed in the previous section, comparing all substrates the Klarite 308 was expected to show best overall SERS sensing performance. Also, it can be seen that there was no real trending observed with the 633 nm laser data, specifically while the data did demonstrate that the Klarite 308 outperforms other substrates, the changes in sensing capabilities were not substantial. This implies that there might be other parameters beside plasmon absorbance locations affecting overall SERS enhancing capabilities, future studies will be conducted.

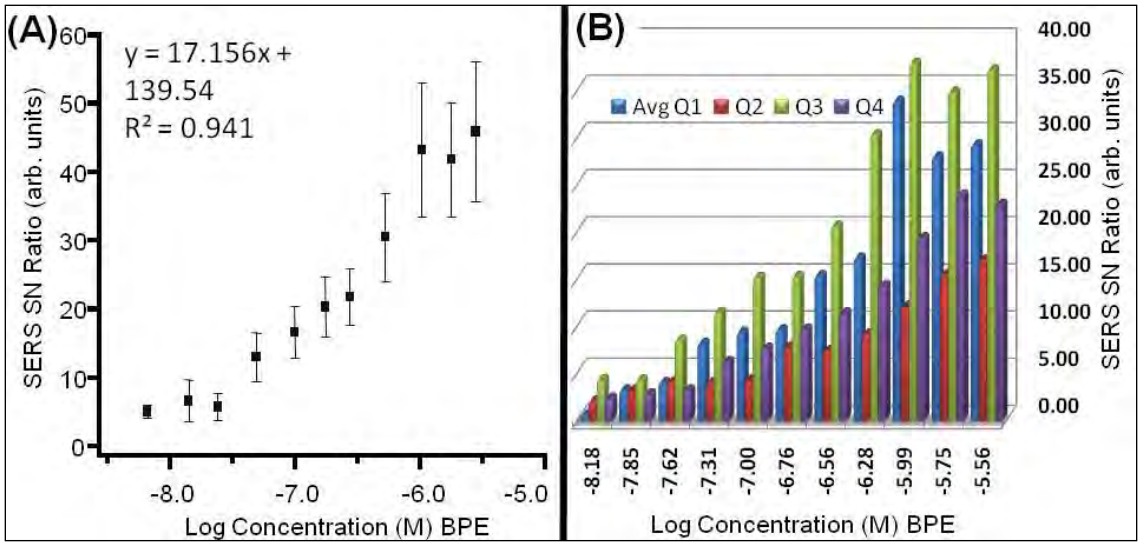

Figure 4. (A) Example of results from a standard Klarite substrate, collected with 785 nm laser, averaged data points with SN >3, error represents 1 std. dev. In this data set the R^2 value observed is 0.941. (B) Example average signal to noise ratios for different quadrants of Klarite 309. Quadrant 3 (Q3) is shown to have the overall highest SERS sensing capabilities.

Table 2. Comparison of standard Klarite, Klarite 308 and Klarite 309 quadrants as determined by SEM analysis and sensitivity determination at 633 nm and 785 nm.

Substrate Type	Plasmon location	Well Width (nm)	Total area overall per pyramid (m^2)	Active area per pryamid (m^2)	Sensitivity @ 785 nm laser excitation (BPE)	Sensitivity @ 633 nm laser excitation (BPE)
Klarite 302	577, 749	1470	4.16E-12	2.16E-12	1.99E-08	5.83E-09
Klarite 308	590, 675	454	4.05E-13	2.07E-13	9.46E-13	6.27E-10
Klarite 309 Q1	723, 840	581	5.75E-13	3.37E-13	5.40E-08	1.98E-09
Klarite 309 Q2	700, 831	484	6.50E-13	2.34E-13	1.99E-08	2.88E-08
Klarite 309 Q3	734, 845	661	6.25E-13	4.37E-13	6.89E-09	2.16E-09
Klarite 309 Q4	713, 836	565	6.50E-13	3.19E-13	2.31E-08	1.97E-09

3.3 Biological sample evaluation

For Army relevant use, SERS substrates must be sensitive to chemical analytes, and also be able to be used for a range of biological samples. Bacteria and spores are just one example of the type of sample for which rapid identification would be advantageous, specifically being able to differentiate between harmful and benign species. In theory, different species of the same type of bacteria have slight differences in their outer wall composition. As SERS is a near-field technique, spore samples coming into contact with the surface should only have the outer wall (1-2 nm from the surface) measured with SERS. Therefore, it should be possible to differentiate between different types of spore samples.

As biological samples remain some of the more challenging analytes due to their complex nature and low Raman cross-sections, the detection capabilities of a standard Klarite and the next generation Klarite substrates were evaluated with the spore sample *B. coagulans*. In these experiments different substrates and the changes in overall band intensity were evaluated.

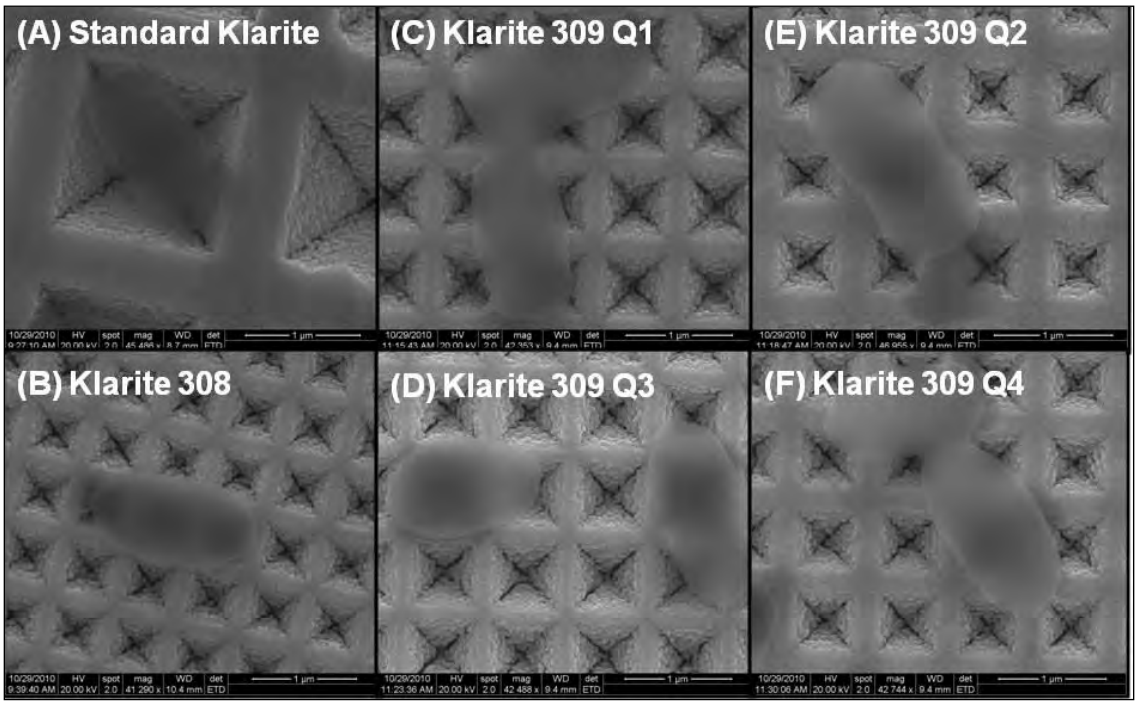

Figure 5. SEM images of spore sample on different Klarite substrate types. Notice the dramatic difference in size between the spore and the active areas on the Klarite surface.

For these experiments an aliquot of the common bacillus spore *B. coagulans* was drop dried onto the substrate SERS active surface. As the sample dried, the spores arbitrarily oriented across the surface, see Figure 5A-F for an examples of spore interactions with the multiple SERS substrate surfaces. As can be seen in Figure 5A, the spore is sitting inside the well. In Figures 5B-F, the spore sits across the SERS surface, thereby proving a significant challenge for sensing. As the spore is a rather large biological sample, its interaction with the surface is going to be limited to the areas where it comes into contact with the SERS surface.

The resulting spectra from the spore sample were collected from five different spots across the surface, see Figure 9B. As can be seen in Figure 6, the spectra all appear fairly consistent, with a main triplet band located at around 1000 cm^{-1}. For the purpose of this article, band identification is not discussed. From these results it can be concluded that the different substrate types demonstrate similar ability to detect the sample. Additionally, there are no obvious changes in overall band intensity suggesting that the different contact and interaction between the spore sample and surface does not have a dramatic effect on overall SERS enhancement. It can be concluded from these results that most likely for larger biological samples, some sort of chemical surface modification to these substrates might be necessary to better capture

and enhance overall signal. Alternatively using a completely different flexible substrate is also to be considered when detecting large biological surfaces.

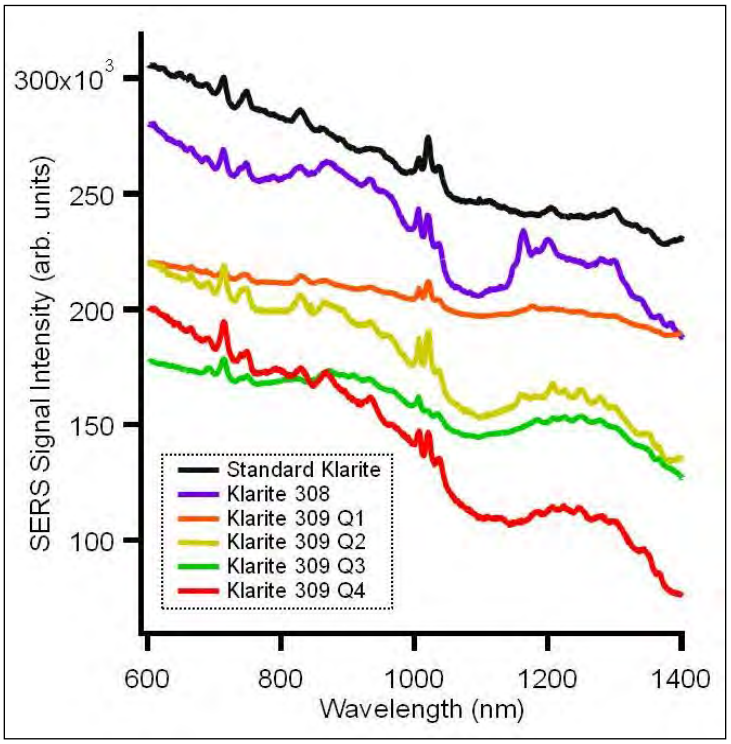

Figure 6. Example spectra collected from spore samples on different types of Klarite substrates.

4. CONCLUSIONS

In this paper, characterization and comparison of the next generation Klarite substrates 308 and 309 to the standard Klarite substrate has been shown for different excitation wavelengths. From the characterization results looking at a common SERS active analyte it can be concluded overall that the next generation Klarite substrate's SERS sensing performance is significantly better, up to four orders of magnitude in some cases. Future works will focus on AFM analysis to determine actual sensing area, testing next generation Klarite response to energetic samples and modeling efforts to determine hot spot location across a substrate surface, and extension to other analyte systems. Additionally, as these substrates are optimized and made more market ready, we expect to re-evaluate their sensitivity and reproducibility.

ACKNOWLEDGEMENTS

Thank you to Renishaw Diagnostics for multiple discussions regarding the response of the next generation Klarite substrates, and for the opportunity to evaluate a potential new product line.

REFERENCES

[1] Hankus, M.E., Cullum, B.M., "SERS probes for the detection and imaging of biochemical species on the nanoscale," Proceedings of the SPIE - The International Society for Optical Engineering, 638004-638001-638012 (2006).
[2] Hankus, M.E., Cullum, B.M., "SERS nanoimaging probes for characterizing extracelllar surfaces - art. no. 675908," Smart Biomedical and Physiological Sensor Technology V, 75908-75908 (2007).
[3] Hankus, M.E., Gibson, G., Chandrasekharan, N., Cullum, B.M., "Surface-enhanced Raman scattering (SERS) - nanoimaging probes for biological analysis," Smart Medical and Biomedical Sensor Technology Ii, 106-116 (2004).

[4] Hankus, M.E., Gibson, G.J., Cullum, B.M., "Characterization and optimization of novel surface-enhanced Raman scattering (SERS)-based nanoimaging probes for chemical imaging," Proceedings of the SPIE - The International Society for Optical Engineering, 600704-600701-600711 (2005).
[5] Hankus, M.E., Li, H.G., Gibson, G.J., Cullum, B.M., "Surface-enhanced Raman scattering-based nanoprobe for high-resolution, non-scanning chemical imaging," Analytical Chemistry, 7535-7546 (2006).
[6] Hankus, M.E., Stratis-Cullum, D.N., Pellegrino, P.M., "Towards Advanced Biological Detection using Surface Enhanced Raman Scattering (SERS)-based Sensors," Biosensing Iii, (2010).
[7] Kneipp, K., Kneipp, H., "Detection, identification, and tracking of biomolecules at the single molecule level using SERS," Biophysical Society, (2005).
[8] Kneipp, K., Kneipp, H., "Single Molecule Raman Scattering," Appl. Spectros., 322A (2006).
[9] Kneipp, K., Kneipp, H., Dasari, R.R., Feld, M.S., "Single molecule Raman spectroscopy using silver and gold nanoparticles," Indian Journal of Physics and Proceedings of the Indian Association for the Cultivation of Science-Part B, 39-47 (2003).
[10] Hankus, M.E., Stratis-Cullum, D.N., Pellegrino, P.M., "Characterization of next-generation commercial surface-enhanced Raman scattering (SERS) substrates " Proc. SPIE, 80180P (2011).
[11] Holthoff, E.L., Stratis-Cullum, D.N., Hankus, M.E., "Xerogel-Based Molecularly Imprinted Polymers for Explosives Detection," Chemical, Biological, Radiological, Nuclear, and Explosives (Cbrne) Sensing Xi, (2010).
[12] Holthoff, E.L., Stratis-Cullum, D.N., Hankus, M.E., "A Nanosensor for TNT Detection Based on Molecularly Imprinted Polymers and Surface Enhanced Raman Scattering," Sensors, 2700-2714 (2011).
[13] Holthoff, E.L., Stratis-Cullum, D.N., Hankus, M.E., Pellegrino, P.M., "ANYL 57-Nanosensor for explosives' detection based on molecularly imprinted polymers and surface enhanced Raman scattering," Abstracts of Papers of the American Chemical Society, 57-ANYL (2009).
[14] Jian, S., Hankus, M.E., Cullum, B.M., "SERS based immuno-microwell arrays for multiplexed detection of foodborne pathogenic bacteria," Proceedings of the SPIE - The International Society for Optical Engineering, 73130K (73110 pp.) (2009).
[15] Guicheteau, J., Argue, L., Emge, D., Hyre, A., Jacobson, M., Christesen, S., "*Bacillus* Spore Classification via Surface-Enhanced Raman Spectroscopy and Principle Component Analysis," Applied Spectroscopy, 267-272 (2008).
[16] Li, H., Baum, C.E., Sun, J., Cullum, B.M., "Multilayer enhanced SERS active materials: fabrication, characterization, and application to trace chemical detection," SPIE, 621804 (2006).
[17] Li, H., Patel, P.H., Cullum, B.M., "Novel multilayered SERS substrates for trace chemical and biochemical analysis," SPIE, (2004).
[18] Alexander, T.A., "Applications of Surface-Enhanced Raman Spectroscopy (SERS) for Biosensing: An Analysis of Reproducible, Commercially Available Substrates," SPIE, 600703 (2005).
[19] Alexander, T.A., "Development of Methodology Based on commercialized SERS-active Susbtrates for Rapid Discrimination of Poxviridae Virions," Anal. Chem., 2817-2825 (2008).
[20] Alexander, T.A., Le, D.M., "Characterization of a commercialized SERS-active substrate and its application to the identification of intact Bacillus endospores," Appl. Opt., (2007).
[21] Alexander, T.A., Pellegrino, P.M., Gillespie, J.B., "Near-Infrared Surface-Enhanced-Raman-Scattering-Mediated Detection of Single Optically Trapped Bacterial Spores," Applied Spectroscopy, 1340-1345 (2003).
[22] Netti, M.C., Zoorob, M.E., Charlton, M.C.B., Ayliffe, P., Mahnkopf, S., Stopford, P., Todd, K., Lincoln, J.R., Perney, N.M.B., Baumberg, J.J., "Probing molecules by Surface-Enhanced Raman Spectroscopy," SPIE, (2006).
[23] Perney, N.M.B., Baumberg, J.J., Zoorob, M.E., Charlton, M.E.B., Mahnkopf, S., Netti, C.M., "Tuning localized plasmons in nanostructured substrates for surface-enhanced Raman scattering," Optics Express, 847-857 (2006).
[24] Hankus, M., Stratis-Cullum, D., Pellegrino, P., "Enabling Technologies for Point and Remote Sensing of Chemical and Biological Agents Using Surface Enhanced Raman Scattering (SERS) Techniques," ARL Technical Report, 132 (2009).

1 ADMNSTR
DEFNS TECHL INFO CTR
ATTN DTIC OCP
8725 JOHN J KINGMAN RD STE 0944
FT BELVOIR VA 22060-6218

18 US ARMY RSRCH LAB
ATTN IMNE ALC HRR
MAIL & RECORDS MGMT
ATTN RDRL CIO LL TECHL LIB
ATTN RDRL CIO MT TECHL PUB
ATTN RDRL SED D M HANKUS (15 HCS)
ADELPHI MD 20783-1197

INTENTIONALLY LEFT BLANK.